EDDY CURRENT LOSSES

MAGNETIC CORE LOSSES

The magnetic core of an electrical machine is magnetized by a constant (dc) magnetic field or an alternating (ac) field. When an ac magnetic field is applied the material is magnetized by internal rearrangement of magnetic domains in complex processes which cause eddy currents to flow in the material. These eddy currents cause heat to be dissipated, and this is referred to as the magnetic core loss or iron loss. The magnetic core is designed to amplify and control the direction of the magnetic flux which in turn determines a machine's performance, whether it is a transformer, motor, generator, or other electromagnetic device. The magnetic cores of most electrical machines subjected to ac magnetization are assembled from thin steel laminations or wound from thin steel strip to limit the losses. The material is commonly referred to as electrical or electrotechnical steel. Magnetic core loss is important for two reasons. First, it has an important role in machine design because the heat it produces must be safely dissipated without deterioration of performance or cause a risk of failure due to local overheating or thermal cycling. Second, magnetic core loss represents a vast amount of waste energy throughout the world. Although electrical machines such as transformers can be over 98% efficient, the cost of the losses over a machine's lifetime can far exceed its capital cost. Added to this, it is estimated that core loss in distribution transformers and large motors costs over 2 billion dollars per annum in the United States alone. The importance of magnetic core loss to environmental protection can be judged from the fact that around 5% of all electricity generated is wasted by being converted into heat in magnetic cores.

This article focuses on magnetic core losses occurring in electrical steels used in power applications, because in volume and economic terms this is by far the most important magnetic material used in power devices. However, it should be mentioned that magnetic core losses are also important in nickel-iron, cobalt-iron, ferrites, and amorphous magnetic materials used in far smaller volumes, mainly at magnetization frequencies greater than 50 Hz to 60 Hz. Much of the content of this article generally also applies to these other materials and their industrial applications but interested readers should refer to more specific works such as Refs 1–3.

ELECTRICAL STEELS

Electrical steels typically 0.15 mm to 0.65 mm thick form the cores of electrical machines where the magnetic flux varies and hence magnetic losses occur. They can be conveniently divided into two main groups; non-oriented steels used mainly in motor applications and grain-oriented steels used mainly for transformer cores. Non-oriented steels contain up to around 2.7% silicon (balance iron) and are supplied semiprocessed, where the user gives a final heat treatment to develop the magnetic properties, or in the fully processed condition where the material is ready to build into cores. Grain-oriented steels contain around 3.2% silicon and by a complex production process have optimum magnetic properties when magnetized along one particular direction (the rolling direction of the strip). Their magnetic properties when magnetized along the rolling direction are far superior to those of non-oriented steels but their strong directional properties also limit their use. Non-oriented steels are cheaper than grain-oriented steels because of the simpler manufacturing process.

It should be mentioned that other materials such as high silicon alloys, iron-based amorphous material, and nanocrystalline alloys are used in some applications at power frequencies. They are not dealt with here but more detail can be found in Ref 4.

Non-oriented Electrical Steels

Non-oriented electrical steel is typically produced in strips up to 1300 mm wide and in thickness from 0.35 mm to around 0.65 mm. Its magnetic properties are almost isotropic, that is almost independent of magnetizing direction in the plane of the sheet. Although non-oriented steels are usually discussed as if they were completely isotropic they all show varying degrees of anisotropy depending on the processing and composition. The material is almost always covered with a thin insulating layer designed to provide electrical insulation between adjacent sheets in a stacked core. The choice of coating is also important in punching and welding performance of the steel.

Silicon is added to non-oriented steels in order to increase the electrical resistance which in turn reduces the magnetic losses. Magnetostriction, an important cause of acoustic noise in magnetic cores, also decreases with increasing silicon content. These benefits are traded off against a reduction in saturation magnetization as shown in Fig. 1. The silicon content is limited to just over 3.4% due to brittleness of high silicon alloys although it is possible to use alternative manufacturing routes to increase this value. Because of the effect of silicon on their magnetic properties, non-oriented alloys tend to have either low silicon content with high core loss and high permeability or high silicon content with lower core loss and permeability. The challenge to manufacturers is to produce high permeability, low loss material with adequate mechanical properties at an economic cost.

Grain-Oriented Electrical Steel

The magnetic and physical properties of single crystals of silicon-iron alloys are highly anisotropic and this is put to good use in grain-oriented electrical steel. Silicon-iron alloys have a body centered cubic crystalline atomic structure with a so-called easy direction of magnetization along the cube edge {100} directions. By a suitable combination of cold rolling and heat treatment a large proportion of grains having {001} directions close to the rolling direction of silicon-iron strip can be formed (4). Figure 2 shows a schematic representation of grains in grain-oriented silicon-iron sheet. Typical permeability and loss characteristics are shown in Fig. 3. Grain-oriented silicon-iron is often referred to as [001](110) oriented silicon steel or Goss textured silicon steel (named after the inventor

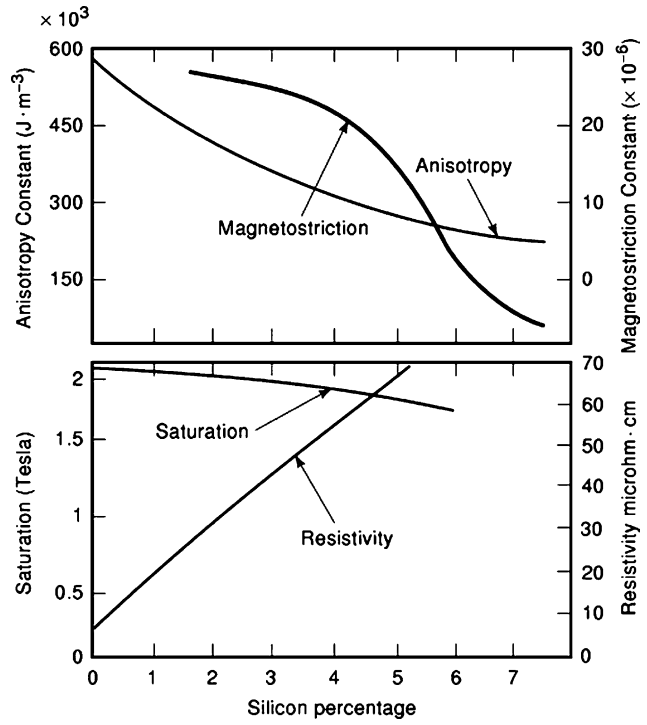

Figure 1. Variation of properties of iron alloys with silicon content.

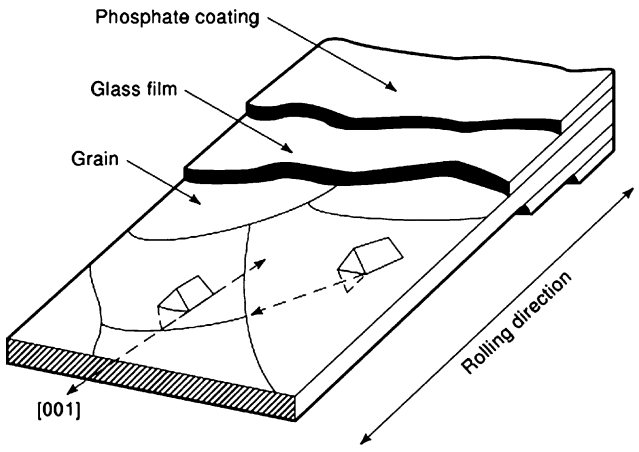

Figure 2. Schematic representation of grain-oriented electrical steel sheet.

N.P. Goss). The alloy usually contains about 3.2% silicon by weight.

A crucial factor in developing good magnetic properties is to control the impurity level during the steel production process. Certain impurities such as manganese sulfide (MnS) or aluminum nitride (AlN) are needed in the development of the [001](110) texture so they must be removed in a subsequent anneal. The steel strip is coated with a thin magnesium oxide layer which reacts with the steel during a high temperature anneal to form a glass film or Forsterite layer. A final phosphate coating is applied which not only provides the insulation needed in laminated stacks, strip or wound cores but also produces a tensile stress along the rolling direction of the steel. This has a beneficial effect

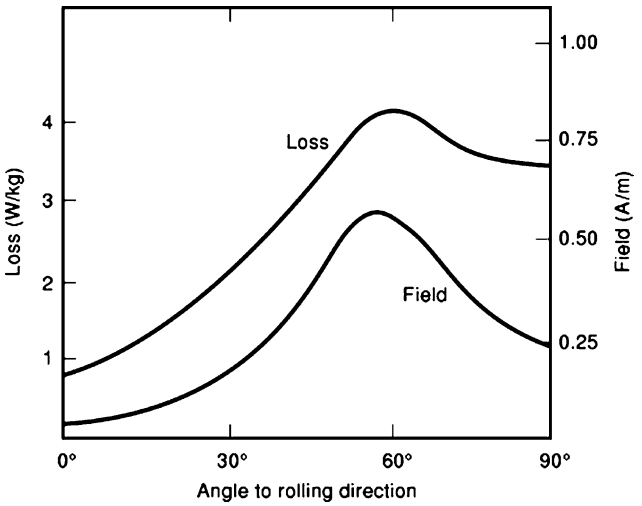

Figure 3. Deterioration of power loss and permeability of grain-oriented silicon steel with direction of magnetization relative to the rolling direction.

on the magnetic properties and reduces magnetic losses in practice.

There are two groups of grain-oriented silicon steels commercially available, conventional material and high permeability material. The high permeability material is produced by a different processing route to develop a texture with a large proportion of grains close to the ideal [001](110) orientation. It has higher permeability and lower losses than the conventional material partly due to the improved texture and partly due to the presence of a higher beneficial coating induced stress.

The high permeability steel has relatively large grains up to around 1 cm in diameter which tends to have an adverse effect on the magnetic properties because of the presence of wide domains. The losses of this material can be further reduced by 5% to 10% by one of a variety of surface treatment techniques which cause so-called domain narrowing or refinement to take place (5). This process makes the magnetic domains narrower with a resultant reduction in losses when magnetization takes place along the rolling direction.

DOMAIN STRUCTURES IN ELECTRICAL STEELS

In order to understand the magnetic characteristics of electrical steels and to identify areas of potential development it is necessary to have an understanding of their magnetic domain structures. Magnetic domains are regions in which all the atomic magnetic moments are aligned parallel so each domain is similar to a tiny magnet. In silicon-iron the magnetic moments within single domains are almost always oriented along {100} directions because of high magnetocrystalline energy which is developed if the moments are aligned along any other direction. This does occur in the regions between adjacent domains referred to as domain walls which are only hundreds of atoms thick. The walls lie between domains whose atomic moments, and hence magnetization, lie at 90° or more commonly 180° to each other.

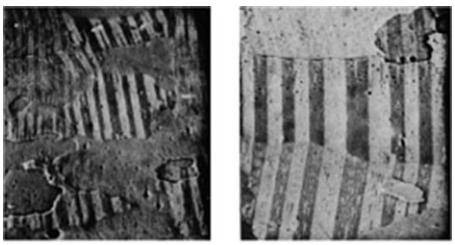

Figure 4. Typical domain structures in grain-oriented silicon steel: (a) narrow domains in small grain material, (b) wide domains in large grain material (rolling direction vertical).

A detailed review of domain structures in grain-oriented silicon-iron is given in reference (6).

A typical domain pattern observed on a surface of grain-oriented silicon-iron sheet is shown in Fig. 4. The wide dark and light areas are domains whose magnetizations are opposite to each other and separated by 180° walls. The effect of a grain boundary and slightly misoriented grains is also seen but the main volume of the steel is made up of bar domains running almost parallel to the rolling direction of the sheet. These main domains also completely penetrate the material so patterns on either surface are very similar.

When an external magnetic field is applied parallel to the rolling direction magnetization occurs by the relative volumes of *dark* and *light* domains changing as the domain walls move through the material. At a sufficiently high external field level all the domains oriented in one direction will have disappeared and a single domain is left. This condition is magnetic saturation. If the external field is applied at an angle to the rolling direction in the plane of the sheet, magnetization will be more difficult and domains oriented along [010] and [100] will have to expand in volume (from an initial small fraction). This is a far more lossy process and a higher magnetic field will be needed so the bulk magnetic characteristics will be similar to those shown in Fig. 3.

When magnetic domain walls move through the steel sheet electromotive forces (emfs) are induced opposing the motion of the walls and creating eddy currents which are the source of the I^2R core loss occurring under ac magnetization.

The magnetic domain distribution in non-oriented steels is far more complex than in grain-oriented steels due to the much smaller grain size and the random distribution of grain orientation. However, the same type of loss producing domain wall motion occurs under ac magnetization.

LOSSES IN THIN LAMINATIONS

Magnetic losses occur in thin laminations as a result of domain wall motion. Internal emfs, fields, and eddy currents associated with domain wall motion cause the electrical energy to be converted into heat energy through the magnetic field. In electrical steels the core loss is broken down according to:

$$P = P_h + P_e + P_a \tag{1}$$

Here the total loss, P, of a lamination is expressed in J/kg and represents the loss per cycle of magnetization. P_h represents hysteresis loss which is assumed to be independent of magnetizing frequency. It is determined from the area of the dc B-H loop. The B-H loop is the representation of the relationship between *flux density* B and *magnetic field* H at any instant in time. P_e is the classical eddy current loss calculated from Maxwell's theory (7) on the assumption that the B-H characteristic is linear (permeability constant) and the flux density varies sinusoidally with time, it ignores the presence of magnetic domains. P_a represents the remainder of the loss which is attributed to the rapid motion of domain walls. All three components increase with increasing peak flux density and with frequency (hysteresis loss per cycle is assumed to be independent of frequency).

The hysteresis loss is mainly a function of the level of purities, grain orientation, and internal stress. The size, shape, and distribution of impurities have a complex effect on the magnitude of the hysteresis loss but generally impurities 0.001 mm to 0.0001 mm diameter are most harmful. Hysteresis loss tends to increase with decreasing lamination thickness particularly in grain-oriented steels where surface roughness or coatings become relatively higher in thin materials.

The classical eddy current loss is often written as,

$$P_\mathrm{e} = \frac{(\pi B f d)^2}{6\rho} \tag{2}$$

where B is the peak value of the sinusoidal flux density, f is the magnetizing frequency, d is the sheet thickness, and ρ is the electrical resistivity of the steel. High resistivity (obtained by addition of silicon) reduces the classical eddy current loss. The fact that P_e depends on d^2 illustrates the need to use thin laminations. Inside the sheet the magnetic field H, flux density B, and localized eddy current loss vary in a complex manner in space and time. Eddy currents near the sheet surfaces tend to shield the inner part of the sheet such that B and H decrease towards the center of a lamination when magnetized under ac conditions. This is more pronounced at higher frequency. The effect is quantified in terms of the depth of uniform magnetization δ defined as the thickness of each of two layers, one on either side of the sheet, which if uniformly magnetized to the magnitude of the surface flux density B_s would give the same effective total flux as that in the whole sheet. δ can be expressed in an approximate form as:

$$\delta = \left(\frac{\rho}{2\pi f \mu}\right)^{1/2} \tag{3}$$

where μ is the permeability of the sheet (assumed constant).

At power frequency, in silicon-iron alloys δ is of the order of 0.15 mm, showing that theoretically full flux penetration occurs in steel around 0.3 mm thick.

The anomalous loss P_a was often referred to as the excess eddy current loss because it also originates from eddy currents. (It should be noted that even the hysteresis loss

P_h is caused by microeddy currents and that today P_a is often regarded as being hysteretic in nature.) The proportion of anomalous loss is expressed as the anomaly factor η.

$$\eta = \frac{(P_a + P_e)}{P_e} \tag{4}$$

The anomaly factor in electrical steels is typically 2 to 5, but it increases in very thin strips and in 0.02 mm thick amorphous magnetic material η can be higher than 100, which throws further doubt on the underlying physical principles on which Eq. (1) is based. The hysteresis loss accounts for 30% to 50% of the loss of low silicon steel, the classical eddy current loss accounts for 40% to 60%, and the excess eddy current loss accounts for 10% to 20% of the total loss. In higher silicon steels the hysteresis loss is proportionately larger (50% to 70%) because the classical eddy current loss decreases (20% to 30%) due to the increased resistivity. The excess eddy current loss remains around the same proportion.

Much of the cause of the anomalous loss can be understood by considering a grain oriented steel with 180° bar domains as in Fig. 4. When magnetized along the rolling direction the domain walls are expected to move ideally in a linear fashion at the same frequency as the applied magnetic field. However, each wall, which in the demagnetized state is assumed to be planar and normal to the sheet, moves faster on the steel surface than in the interior and consequently moves further on the surface. This causes an eddy current shielding action and the volume of each wall also increases. The net effect of this domain wall bowing phenomenon is to increase the eddy current loss by making a large contribution to P_a. Other contributing components of P_a are simply due to the approximations made in calculating P_e by neglecting the nonlinear B-H characteristic of the material. In an ideal grain in polycrystalline grain-oriented steel the anomaly factor η can be calculated from:

$$\eta = 1.63\frac{a}{d} \tag{5}$$

where a is the average domain width in the demagnetized state. High permeability grain-oriented material has larger grain size associated with the formation of improved [001](110) texture. These grains have wider domains than in conventional material so a part of the benefit of the improved orientation is lost due to a higher anomaly factor. Domain refinement processes referred to earlier are used to reduce the average value of a in large grains by surface treatment and the application of high stress coatings produce beneficial tensile stress in the steel which also has the effect of reducing a.

It can be seen from the preceding discussion that there are some conflicting requirements when attempting to reduce eddy current and hysteresis loss to their minimum levels. At the same time it should be remembered that this is an artificial separation of loss components. To obtain low eddy current loss the material must be thin and have small grain size and it must have a high silicon content. To obtain low hysteresis loss thick material with large grain size is needed with low impurity levels and good surface conditions. These partly conflicting needs lead to a general reduction in losses as thickness decreases to a point where hysteresis loss tends to increase so an optimum thickness does occur with most alloys. The optimum thickness is generally lower than practical commercial thicknesses and for any particular composition it depends on operating flux density and frequency level.

It should be noted that in many applications it is desirable to optimize the permeability of the steel and minimize the loss at the same time. To obtain high permeability in electrical steels low silicon content is desirable combined with small grain size and low impurity levels (8). Thus it is difficult to optimize the two parameters simultaneously but techniques such as domain refinement and application of stress coatings help in this ambition.

Losses Under Distorted Flux Conditions

Electrical steels are developed and graded for sale based on their losses measured at 1.5 T or 1.7 T, 50 Hz or 60 Hz under sinusoidal time varying flux density conditions. Single sheets or Epstein strips are tested in these ways under well defined conditions (9). In practice laminations are often partly magnetized under nonsinusoidal flux conditions. It is convenient in such cases to determine the loss experimentally from:

$$P = \frac{1}{T}\int_0^T h_s \frac{db}{dt} dt \tag{6}$$

where T is the magnetization period, h_s is the instantaneous tangential component of the field at the steel surface, and db/dt is the corresponding instantaneous value of the rate of change of the average spatial flux density within the material. These terms are experimentally obtainable using a variety of standard techniques. In general if

$$b = \sum_{n=1}^{\infty} B_n \sin(\omega n t + \phi_{bn}),\ h = \sum_{n=1}^{\infty} H_n \sin(\omega n t + \phi_{hn}) \tag{7}$$

then it can be shown that:

$$P = \sum_{n=1}^{\infty} f_n \pi B_n H_n \sin(\phi_{bn} - \phi_{hn}) \tag{8}$$

where B_n and H_n are peak values of the respective nth harmonic components. ϕ_{bn} and ϕ_{hn} are the phase angles of the nth harmonic B and H components with respect to an arbitrary reference. Usually it is sufficient to consider odd values of n up to 9 unless the waveform is very distorted as in some electronic systems applications. Eqs. (1) and (8) are numerically identical. However Eq. (8) can be applied without considering its physical interpretation to any normal magnetizing condition found in electrical steels used in power devices. It is very useful for application in modern computerized loss measuring systems.

Other approaches based on physical models have been developed in order to extend the basic loss separation method expressed in Eq. (1) to the case of distorted flux waveforms. Precise methods of predicting iron loss under distorted flux density have been developed (10) but they do need a rigorous knowledge of the order, amplitude, and phase of the flux density harmonics. The approach depends

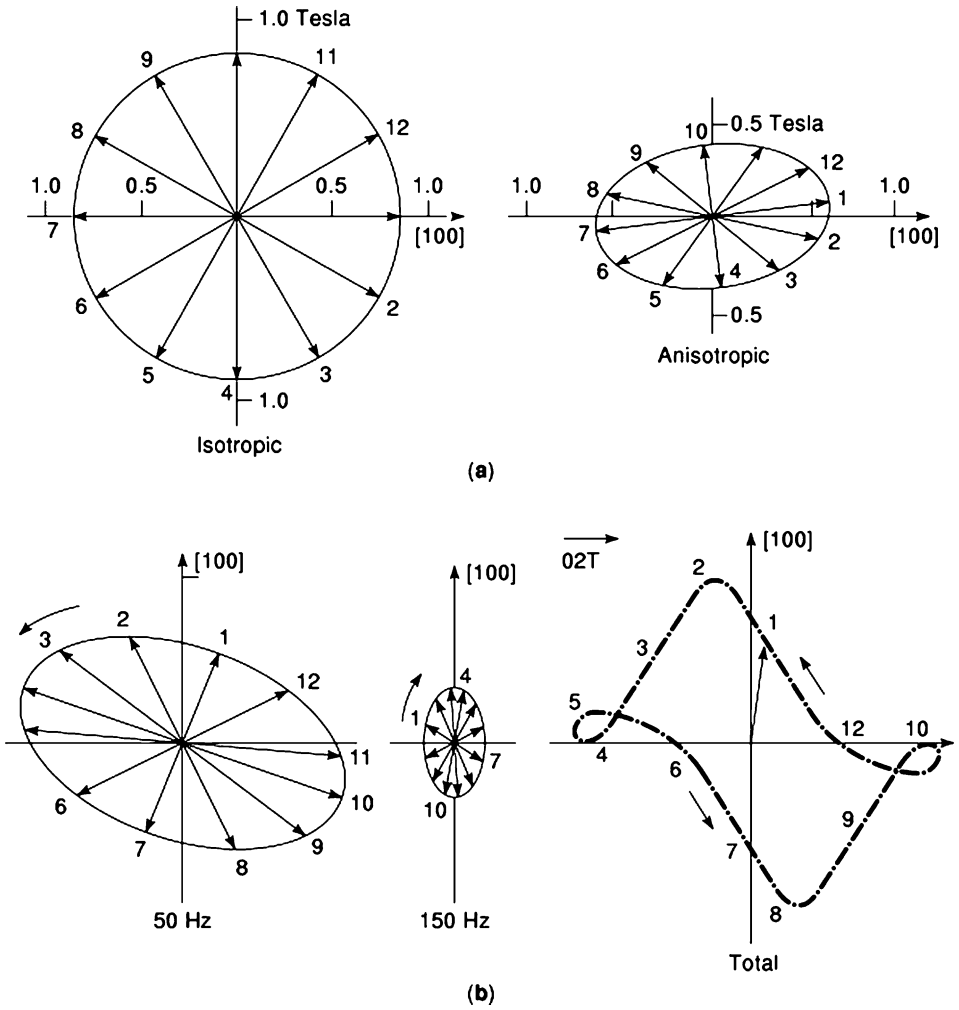

Figure 5. Schematic rotating flux density vectors showing (a) pure and elliptical loci in isotropic and anisotropic steel sheet (b) complexity caused by harmonic distortion in anisotropic material (11).

on an assumption based on generalized experimental and theoretical results that under sinusoidal flux density P_n is proportional to the average rate of change of flux density, P_e is proportional to the square of the average rate of change of flux density, and P_a is proportional to the average rate of change of flux density to the power 1.5. From this the total loss under distorted flux can be calculated with prior knowledge of loss separation at one sinusoidal flux density value. The method is still at a development stage but interestingly it is based firmly on rate of change of flux density which in turn depends upon mean domain wall velocities.

Electrical steels used in motors are increasingly subjected to flux waveforms produced by voltages derived from pulse width modulation (*PWM*) and other electronic sources. The PWM output voltage is obtained by comparing the high frequency carrier with a reference voltage. The modulating waveform determines the inverter output fundamental frequency and its amplitude controls the *rms* (root-mean-square) output voltage. The ratio of the amplitude of the modulating waveform to that of the carrier is the modulation index. The carrier frequency is normally between 1 kHz and 20 kHz so very high harmonics will appear in the output voltage waveform.

Losses in materials subjected to PWM voltage excitation can be 50% higher than under an equivalent sinusoidal voltage. These increases can be explained to some extent from calculations based on modifications to the approach of reference (10) to take into account the more complex waveshapes. The calculations make many approximations and again depend on initial knowledge of magnetic material characteristics but they confirm the expected loss increase.

Losses Under Rotational Magnetizing Conditions

Electrical steels are often subjected to so-called rotational magnetization in machine cores. Pure rotational magnetization is defined as the condition where the flux is of constant magnitude and rotates at constant angular velocity in the plane of a lamination. Fig. 5 shows representations of the phenomenon under different conditions, in Fig. 5(a) a pure rotating flux is depicted as a vector following a circular locus under pure rotational conditions (isotropic material) (11). In the anisotropic case, such as in grain-oriented steel, the rotational flux usually varies in magnitude and angular velocity giving an elliptical locus. The situation is more complex in machine cores where the rotational magnetization can be split into harmonic components as in Fig. 5(b).

Rotational flux causes rotational losses in electrical steels at power frequencies. It is not so common to split ro-

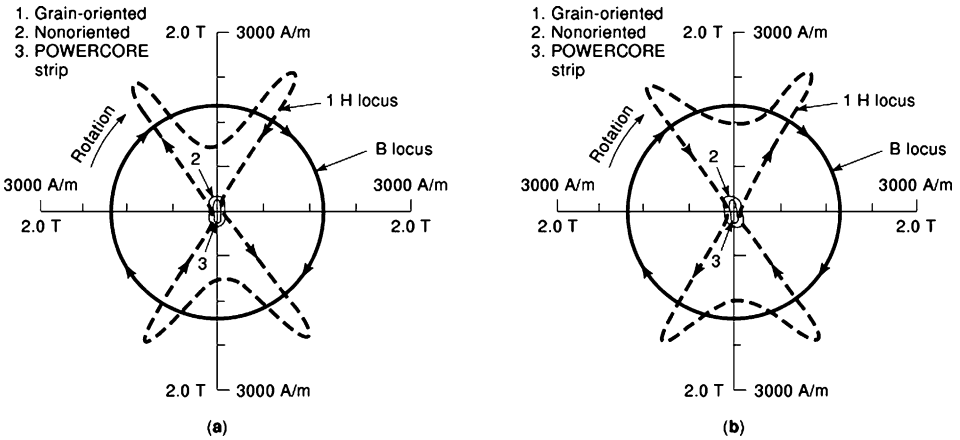

Figure 6. Loci showing small differences of rotating field vectors and large effect of anisotropy under the same peak flux density (1.2 T) for clockwise and anticlockwise rotation (12).

tational loss into hysteresis, eddy current, and anomalous loss components as is normally carried out for unidirectional ac magnetization but the total loss can be obtained from

$$P_r = \frac{1}{T}\int_0^T \left\{ h_x \frac{db_x}{dt} + hy\frac{db_y}{dt} \right\} dt \qquad (9)$$

where h_x and h_y are instantaneous tangential surface field components in orthogonal directions. db_x/dt and db_y/dt are the rates of change of corresponding flux density components. Experimentally the components in Eq. (9) can be obtained using sensors (12). The rotational field variation needed to produce pure rotational flux density is complex in grain-oriented material as shown in Fig. 6. The B locus is circular whereas the instantaneous field variation is very complex due to the high anisotropy of the material and the difficulty of maintaining the flux density constant when the magnetization is along difficult directions in the plane of the sheet.

The losses produced under rotational fields are generally higher than under ac magnetization. Figure 7 shows the variation of rotational loss with flux density in typical electrical steels and amorphous magnetic material (4). At the same flux density the rotational loss is around three times as high as the alternating loss in most steels (magnetized in the easiest direction) apart from at either very low or very high flux density.

Rotational losses are high because associated domain motion necessary for the flux to rotate uniformly and to remain a constant magnitude is very complex. Loss processes such as domain wall nucleation and annihilation and magnetization rotation occur. At very high flux density a single domain is formed so as the magnetization rotates no loss occurs since no domain walls are present and the loss at saturation can be theoretically calculated. This condition does not occur in actual materials because defects will be present which will cause some domain wall formation. It should be noted that the loss under rotational magnetization is not simply the sum of losses which occur when a given material is magnetized separately in two orthogonal directions as might appear to be the case when referring to Eq. (6) and Eq. (9) because, although mathematically the equations are similar, domain wall motion which takes place under rotational magnetization is quite different to

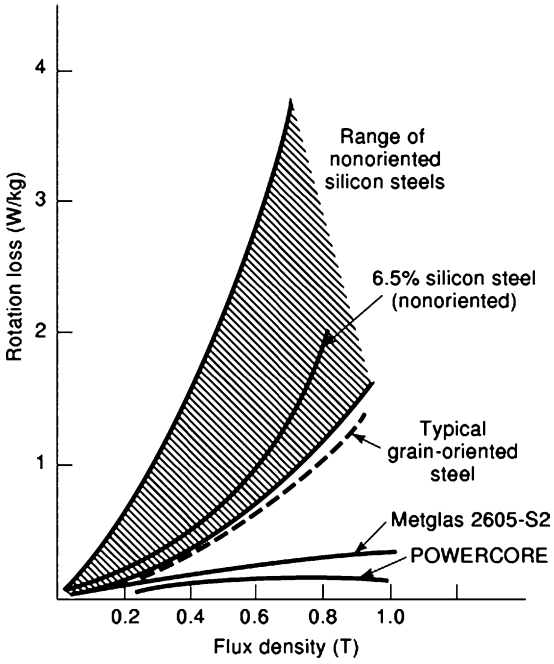

Figure 7. Variation of rotational loss in various materials with flux density (4).

that occuring under unidirectional magnetization

The Influence of Mechanical Stress on Losses

In order to understand the effect of losses due to mechanical stress in electrical steels it is necessary to consider the minimization of free energy in a magnetic alloy. In iron alloys the magnetocrystalline energy dominates and it is extremely high unless the magnetization in each grain is along a {100} direction. Application of a magnetic field introduces more free energy and the domain structure changes to keep the magnitude of the internal energy to a minimum. In this particular case the process of magnetization involves domains reorienting but remaining along {100} directions unless the magnetizing field is very high.

When a mechanical stress is applied to a crystal of cubic material such as silicon-iron magnetoelastic energy, E, is

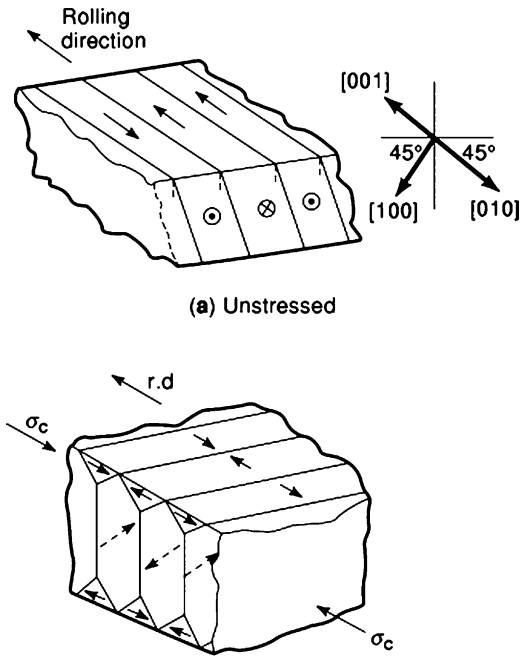

Figure 8. Change of static domain structure in an ideal Goss oriented grain caused by compressive stress along the rolling direction (13).

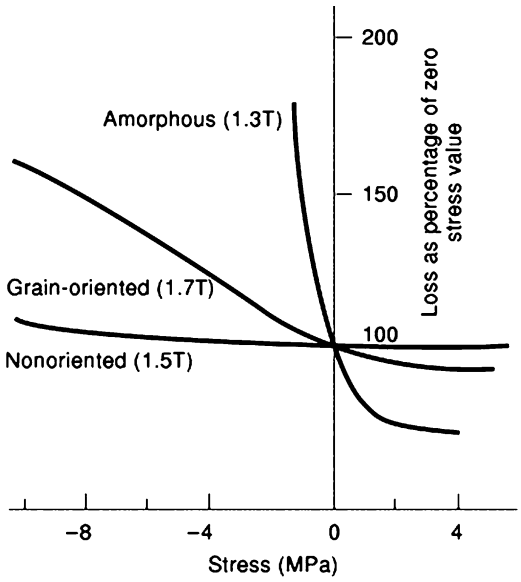

Figure 9. Loss increase under compressive stress in different materials (4).

introduced given by:

$$E = -\frac{3}{2}\lambda_{100}\sigma\left(\alpha_1^2\gamma_1^2 + \alpha_2^2\gamma_2^2 + \alpha_3^2\gamma_3^2 - \frac{1}{3}\right) - 3\lambda_{111}\sigma(\alpha_1\gamma_1\alpha_2\gamma_{2+}\alpha_1\gamma_1\alpha_3\gamma_3 + \alpha_2\gamma_2\alpha_3\gamma_3) \quad (10)$$

where λ_{100} and λ_{111} are magnetostriction constants for the material at a particular temperature, σ is the stress and the direction cosines of the stress and magnetization are $(\alpha_1\alpha_2\alpha_3)$ and $(\gamma_1\gamma_2\gamma_3)$ with respect to the crystal axes.

Figure 8(a) shows an ideal domain structure in a perfectly oriented grain of grain-oriented silicon-iron when no stress is applied. The antiparallel bar domain structure shown in the demagnetized state is primarily due to the high magnetocrystalline energy of the material. Suppose a tensile stress is applied along the [001] direction then in any domain $\alpha_1 = 1$, $\alpha_2 = 0$, $\alpha_3 = 0$, and $\gamma_1 = 1$, $\gamma_2 = 0$, $\gamma_3 = 0$, so Eq. (10) simply reduces to

$$E = -\lambda_{100}\sigma \quad (11)$$

In iron and silicon-iron alloys, λ_{100} is positive so E is negative, showing that the tensile stress reduces the free energy of this domain structure which initially was in a low energy state so the structure remains unchanged. If the material were magnetized along the [001] direction under ac conditions the presence of the stress would have no effect on the loss.

If the stress applied to the structure in Fig. 8(a) is compressive then σ is negative so the free energy expressed by Eq. (11) will be positive and a net energy increase will occur. Typically the magnetoelastic-energy given in Eq. (11) will be of the order of 1% of the total energy dominated by magnetocrystalline energy but it causes a major reorganization of the domain structure to that shown in Fig. 8(b). Here the magnetocrystalline energy is unaffected since all domains still lie along {100} directions but the bulk of the material is now magnetized along the [100] and [010] directions perpendicular to the stress direction and the magnetoelastic energy of these domains is now negative (this can be shown by putting the appropriate values of $\alpha_1\alpha_2\alpha_3$ into Eq. (10)).

The above treatment is an oversimplification of what happens in practice because domain walls, grain boundary interactions, and misorientation of grains are ignored but this process does occur in principle. Obviously if the material is now to be magnetized along the [001] direction the domains oriented along the [100] and [010] directions must rotate through 90° so a far more lossy process occurs.

Figure 9 shows the effect of tension and compression applied along the rolling direction of grain-oriented and non-oriented steels. In the grain-oriented steel tension has a small effect as expected from the previous basic analysis and there is a sharp increase in loss at a certain compressive stress when domains in individual grains take up a structure similar to that shown in Fig. 8(b) in the demagnetized state. Stress applied along the rolling direction of non-oriented steel has a smaller influence on the loss because of the random grain orientation.

If stress is applied along any other direction than the rolling direction, its effect on the domain structure and hence losses can be predicted from Eq. (10). Figure 10 shows how complex stress made up of orthogonal components parallel and perpendicular to the rolling direction can have a wide ranging effect on the losses (14).

In practical laminated cores mechanical stress is very difficult to avoid completely and it is often randomly distributed so its effect on losses cannot easily be accurately quantified. The best method of overcoming the effect of such building stresses is the application of stress coatings referred to earlier which generate a net tensile stress in the

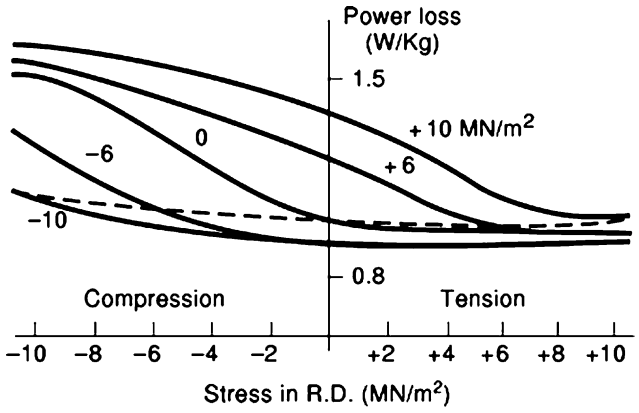

Figure 10. Variation of loss for different combinations of orthogonal stress in grain-oriented steel (1.5 T, 50 Hz). Dotted line shows low sensitivity to isotropic stress (14).

steel along the rolling direction and hence shift the stress sensitivity curves shown in Fig. 9 and Fig. 10 to the right.

FLUX AND LOSS DISTRIBUTION ELECTRICAL MACHINES

Electrical steels are graded according to their performance under ideal conditions of sinusoidal, uniform flux density with no rotational magnetization, or flux perpendicular to the plane of laminations in a stress-free state. When used in a core the magnetization conditions are very complex. Nonuniform flux, flux harmonics, rotational and normal flux, flux deviation from the rolling direction of the sheet, and the influence of temperature and mechanical stress variations all cause additional losses. The deterioration of performance in a core is quantified in terms of the building or destruction factor which is defined simply as the ratio of the per unit core loss of a device to the nominal per unit loss measured under ideal test conditions at the same flux density. In a transformer the building factor varies from just over unity to over 2 depending on the complexity of the core design. The building factor of a motor cannot be defined in the same way because the operating flux density of the steel in a motor varies greatly from point to point so the flux density at which the steel should be magnetized for comparison in the ideal case cannot be defined. However, the deterioration in losses is also very high in motors. It is very difficult to quantify the building factor or the components which contribute to it but in order to attempt to predict its magnitude the internal flux and loss distribution in a core must be known. It is also important to quantify the internal flux and loss distribution to ensure that cores are designed such that laminations are not unnecessarily under or over magnetized and that no local high loss areas occur which can cause material deterioration and ultimate core failure.

There are two approaches which can be taken to determine the flux and loss distribution in a magnetic core. The flux and loss can be measured directly in experimental model cores using arrays of suitable sensors or they can be predicted theoretically based on numerical solution of Maxwell's equations usually using finite element software.

Experimental methods of measuring flux and loss distributions in magnetic cores are tedious and time consuming. Flux distribution is determined from localized measurements made on single laminations in a core. Orthogonal search coils are threaded through small holes drilled in laminations such that the induced voltages in the coils can be used to determine the instantaneous magnitude and direction of flux at a position in the plane of a laminations. The time variation can be shown as series of flux loci derived from arrays of such coils and also presented in terms of the flux harmonics separately. The normal or interlamina flux can be obtained from measurement of voltages induced in small pancake coils on the surfaces of laminations. Apart from being time consuming the core is disturbed by insertion of the sensors which itself can lead to additional experimental errors. Care must be used when scaling up results on small models to predict what happens in larger cores, but on the other hand account is taken of the material properties, airgaps, and other practical characteristics of the core which cannot easily be modeled.

Experimental measurement of localized core loss is based on the principle that the initial rate of rise of temperature of a lamination is proportional to the heat being generated (15). Miniature thermocouples or thermistors are inserted into a core which is energized for a few seconds while the initial temperature rise of a few millidegree centigrade is measured. This technique requires skilled and careful measurements and even then the final uncertainty in the power loss is normally no better than $\pm 5\%$.

Computation methods of determining flux distributions in electromagnetic systems are well advanced in general but predictions in electrical steel cores still need to be treated with care. Although solutions of Maxwell's equations are very accurate they depend entirely on the accuracy and form of the input magnetic material data. In the case of purely isotropic material with no hysteresis the flux distributions can be modeled quite accurately. In the case of anisotropic steel such as grain-oriented steel no method has yet been demonstrated to properly model the anisotropic nature of the B-H characteristics. Often a series of B-H curves obtained from material magnetized at several angles to the rolling direction are used as input data but even this does not take account of the fact that B and H are not collinear in the material unless magnetization is along or perpendicular to the rolling direction (16).

Computational methods of determining flux distribution in laminated cores under ac conditions depend on obtaining a series of solutions corresponding to instantaneous flux distributions at given times in the magnetization cycle from which flux waveforms can be built up. These methods do not take proper account of rotational magnetization processes or spatial differences between B and H directions. Furthermore, in transformer joints in particular, the interlamina flux and air gaps have a major influence on the flux distribution so three-dimensional solutions must be carried out but as yet no programs are available which take proper account of the anisotropy of the material.

Computation of the power loss poses greater problems. It is impracticable to attempt to calculate the power loss

from Eq. (9) so the most common approach is to attempt to calculate the flux density in terms of its magnitude, direction, and harmonic content and to use a look-up table obtained from previous experimental results to estimate the corresponding loss value.

Despite all the difficulties of experimental and computational estimates of flux and loss distributions both have merits depending on the particular device to be investigated. One more practical solution which has become more feasible with the more general use of interactive computing techniques is to combine high speed field computation in a core with a computerized magnetic tester which magnetizes a material under the same field conditions as are computed at each location in the core (17). Such techniques are in their infancy but they could avoid the problem of modelling anisotropic materials magnetized in complex three-dimensional, time varying field situations.

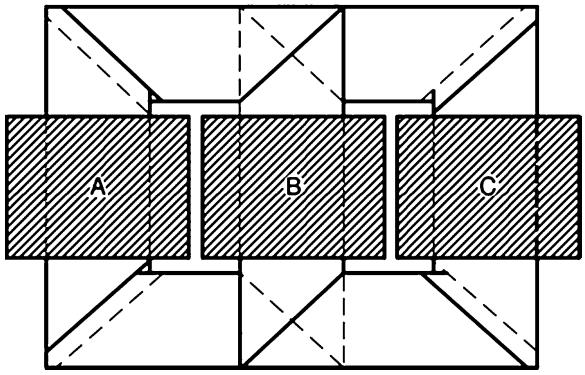

Figure 11. Plan view of 1 layer of laminations in an ideal 3-phase core with primary coils around limbs A, B, C.

Flux and Loss Distributions in Transformers

The flux distribution in a power system transformer depends on the core geometry, the *B-H* characteristics of the core material, the operating flux density, the frequency of magnetization, and the presence of mechanical stress or temperature gradients. Most interest is focused on cores assembled from grain-oriented silicon-iron where the high anisotropy makes the flux remain substantially directed along the rolling direction throughout most of the core volume. Furthermore, the joint areas are of particular interest because in these regions the air gaps, interlaminar flux, and rotational flux can cause high localized losses and are the origin of flux harmonics which can increase the losses in other areas of a core.

Consider the basic 3-phase laminated core geometry shown in Fig. 11. Primary windings A, B, and C produce flux densities of equal magnitude 120° out of phase with each other such that at any instant in time

$$\phi_a = \Phi \sin \omega t, \quad \phi_b = \Phi \sin(\omega t + 120), \quad \phi_c = \Phi \sin(\omega t + 240) \tag{12}$$

where ϕ_a, ϕ_b, ϕ_c are the instantaneous fluxes in limbs A, B, C. Φ is the peak flux and $\omega = 2\pi f$. An ideal flux distribution can be obtained in a simplified form by putting ωt equal to angles from 0° to 180° and calculating the corresponding instantaneous values of ϕ_a, ϕ_b, and ϕ_c. For example, when $\omega t = 0$ there is no flux in limb A and a flux of magnitude 0.866 Φ flows around limbs B and C via the top and bottom yoke.

The practical transformer will be made up of many layers of laminations as shown in Fig. 11 interleaved at the outer four corners and the two inner joints referred to as T-joints. The complex transfer of flux from limb to limb combined with the complex magnetization characteristics of grain-oriented steel makes the actual flux distribution far more complex than inferred from Eq. (12). The localized flux density will be nonsinusoidal in most of the core laminations and this is best described in terms of harmonic flux distributions superimposed on the fundamental distribution expressed ideally by Eq. (12).

Figure 12 shows the theoretical flux distribution in a 5-limb, 3-phase transformer at an instant in time when the

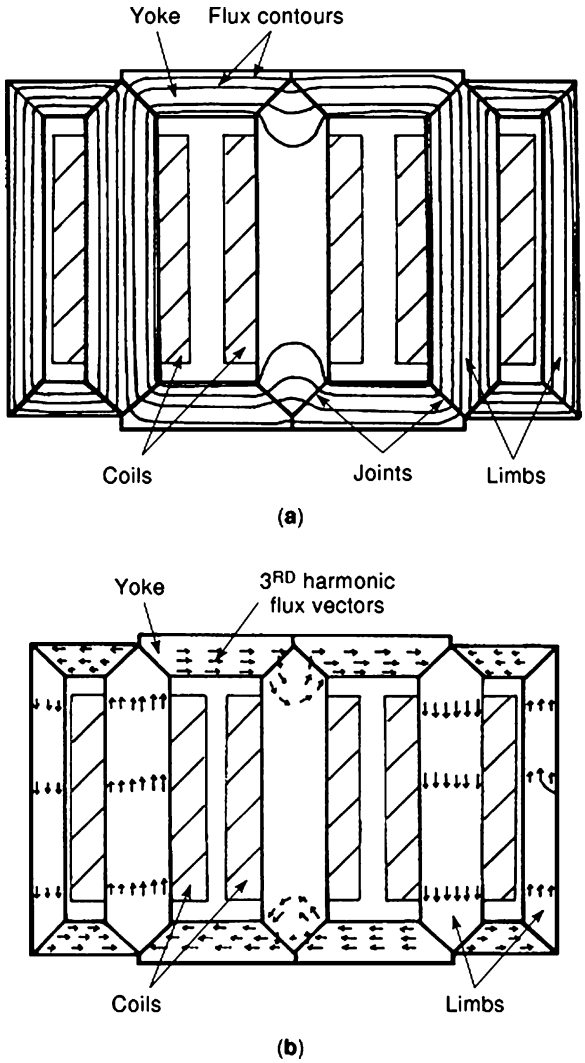

Figure 12. Theoretical flux distribution in a 5-limb, 3-phase transformer core showing flux penetration into the center limb when its coil voltage is zero (a) vector potential (b) 3rd harmonic (B = 1.5 T, 50 Hz) (18).

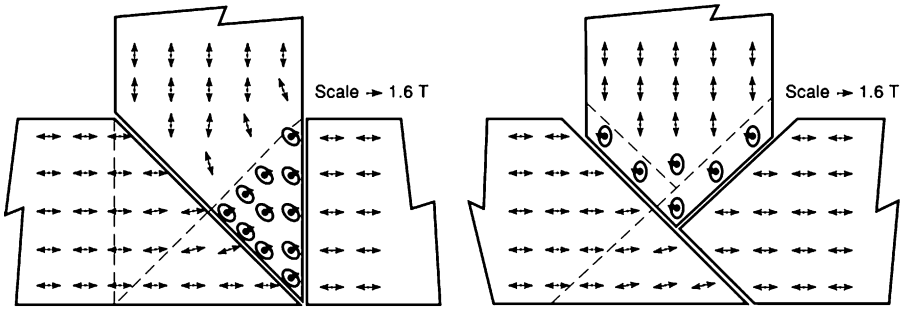

Figure 13. Loci of the 50 Hz component of localized flux density in two common transformer T-joints showing well defined areas of rotational flux (19).

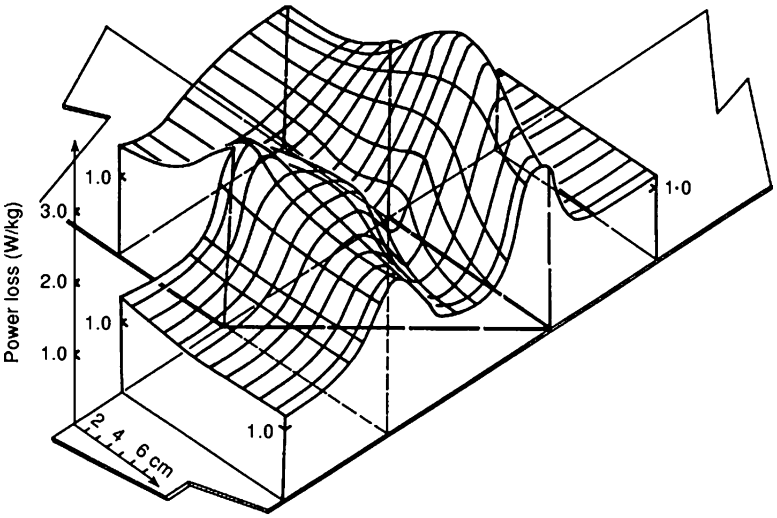

Figure 14. Localized power loss distribution in the 45° to 90° T-joint showing peaks due to normal and rotational flux (1.6 T, 50 Hz) (19).

magnetizing current in the center limb coil (not shown) is zero (the three inner wider limbs carry the coils A, B, and C). Flux penetration into the center limb will be noted (18). Figure 12(b) shows the corresponding direction of the localized 3rd harmonic flux density. Flux in adjacent laminations will be in opposite directions so the total limb flux does not appear to contain any harmonic components.

The T-joint design plays an important role in determining the localized and total core loss of a 3-phase transformer. Figure 13 shows the difference in flux distribution in two commonly used T-joints (19). The locus of the fundamental component of flux density is shown. In both joints the flux remains in the rolling direction of the laminations over most of the area, apart from the region containing the elliptical loci, where rotating flux density occurs. It should be remembered that odd harmonics (up to around the 9th for sinusoidal voltages but much higher for pulsed conditions), which all contribute to the losses, will be superimposed on this distribution. Figure 14 shows the localized loss distribution in one of the cores. The peaks correspond to the regions where the rotational flux occurs and regions where high interlamina flux is present (19). The differences in the flux distributions in this case cause the 45° offset T-joint to have 10% less core loss than the other joint.

The mitered overlap corner joint is most widely used in single phase and three phase laminated cores. The flux remains in the rolling direction apart from in the overlap region itself (20). Figure 15 shows how the regions above and below butt joints are close to saturation. A proportion of flux does go through the high reluctance air gaps at the butt joints and it can be shown that an optimum overlap length gives minimum losses for a particular operating flux density and core size. The flux distribution can be related to the building factor to some extent. The building factor of high permeability steel cores is generally higher than that of cores assembled from conventional grain-oriented steel. This is partly because the uniformity of flux density is greater in cores assembled from the conventional material. At high flux density (greater than 1.7 T) the building factor improves in cores assembled from both types of material as the flux density becomes more uniform closer to saturation.

Measurements made on isotropic and anisotropic cores illustrate the critical importance of the high anisotropy of grain-oriented steels. Figure 16 compares the measured locus of the fundamental components of flux density in cores assembled from grain-oriented silicon-iron and from amorphous magnetic material which is almost isotropic. The flux is far more uniform in the core assembled from the amorphous material and full rotational magnetization occurring at the T-joints ensures uniform flux transfer between yokes and limbs. In this particular T-joint no rotational flux occurs in the grain-oriented steel core and the flux remains in the rolling direction. However, the building factor of the core made from amorphous material is only around 1.1 (provided care is taken to overcome its high stress sensitivity) whereas that of the grain-oriented core of the same geometry at the same flux density is 1.2 to 1.3. This shows that the ideal transformer core material should be isotropic with low rotational losses.

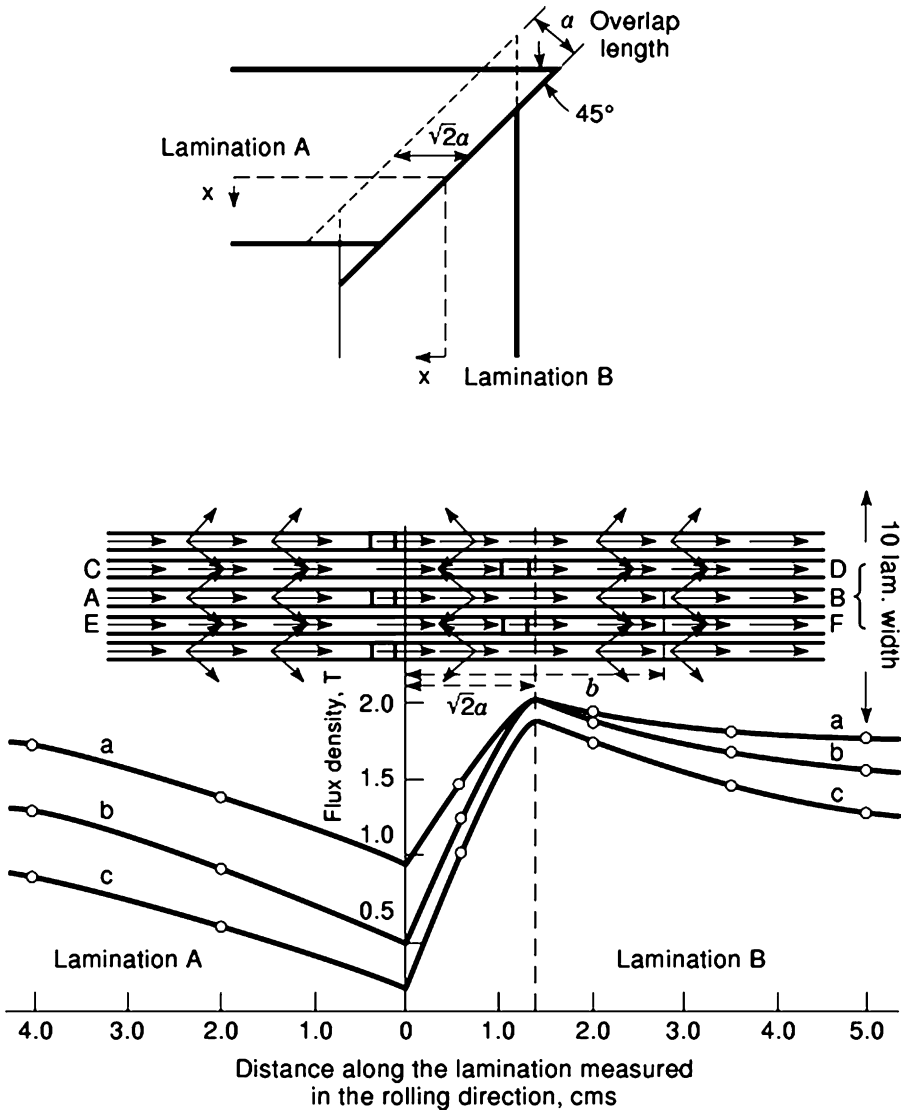

Figure 15. Longitudinal flux density distribution in adjacent laminations in the 45° mitered overlap corner measured at core flux densities of (a) 1.8, (b) 1.5, and (c) 1.1 T, for a 1.0 cm overlap. Saturated regions above and below butt joints are prominent (20).

Limited work has been carried out on wound core transformers. Here the flux mainly remains in separate core paths of the three phase core and very little flux transfers at the intersections between yokes and limbs. This leads to higher harmonic fluxes and a greater dependence of the localized flux and loss distribution on the winding connections.

Flux and Loss Distributions in Motors

Flux and loss distributions in motor cores are controlled by factors similar to those which occur in transformer cores discussed in the last section. Motor cores are generally assembled from non-oriented steel unless the stator core has such a large diameter that segmented cores can be used to minimize losses. In small motors the flux can be assumed to be almost wholly in the plane of laminations of non-oriented steel, so closer agreement is usually found between computed and measured distributions.

Figure 17 shows typical flux distributions measured in the stator or a three-phase induction motor (11). The fundamental and third harmonic flux density loci are separated for convenience and both contain large components of rotational flux behind the teeth and slots. At the core back the flux is mainly low in magnitude and circumferential in direction whereas in the teeth it is high in magnitude and radial in direction.

The loss distribution in a motor core can be easily related to the flux distribution. Losses at the core back are relatively low, behind the teeth and slots where rotational flux occurs the losses are higher and they are highest in the teeth where the flux density is highest. There is typically a factor of 2 to 3 difference between the lowest and highest losses. The actual loss is the sum of the localized losses and by far the largest volume of steel is subjected to rotational flux which accounts for around 25% to 50% of the stator core of a typical induction motor or synchronous generator.

The flux and loss distributions in large motor and generator stators assembled from segments depends on the type of material used (grain-oriented or non-oriented electrical steel) and the stacking method (21). There is only a small difference in the distribution of the fundamental compo-

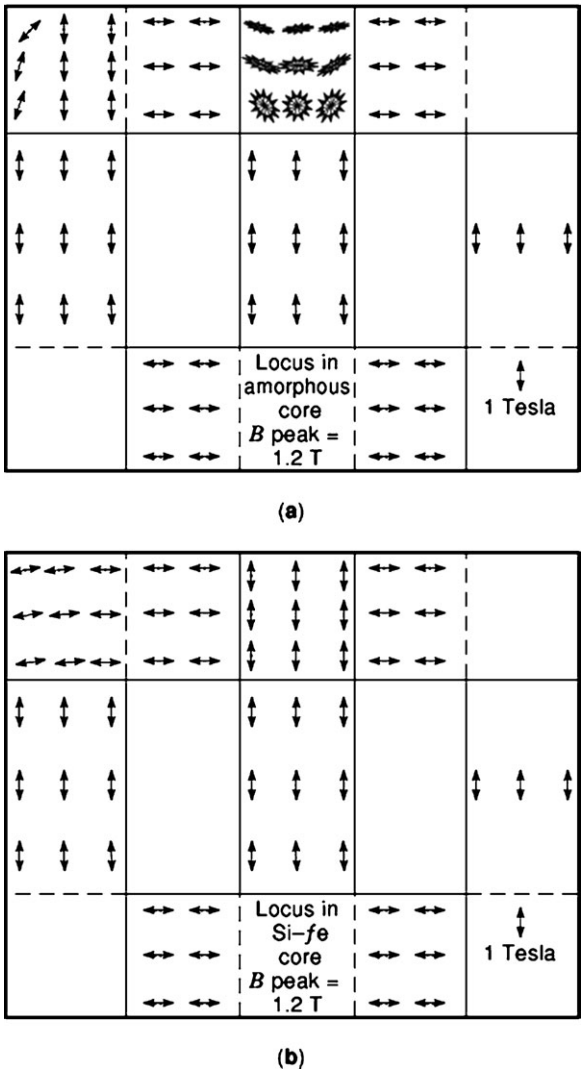

Figure 16. Locus of localized fundamental component of flux density in 3-phase, 3-limb cores assembled from (a) amorphous ribbons and (b) grain-oriented silicon-iron highlighting the large affect of anisotropy (1.2 T, 50 Hz) (11).

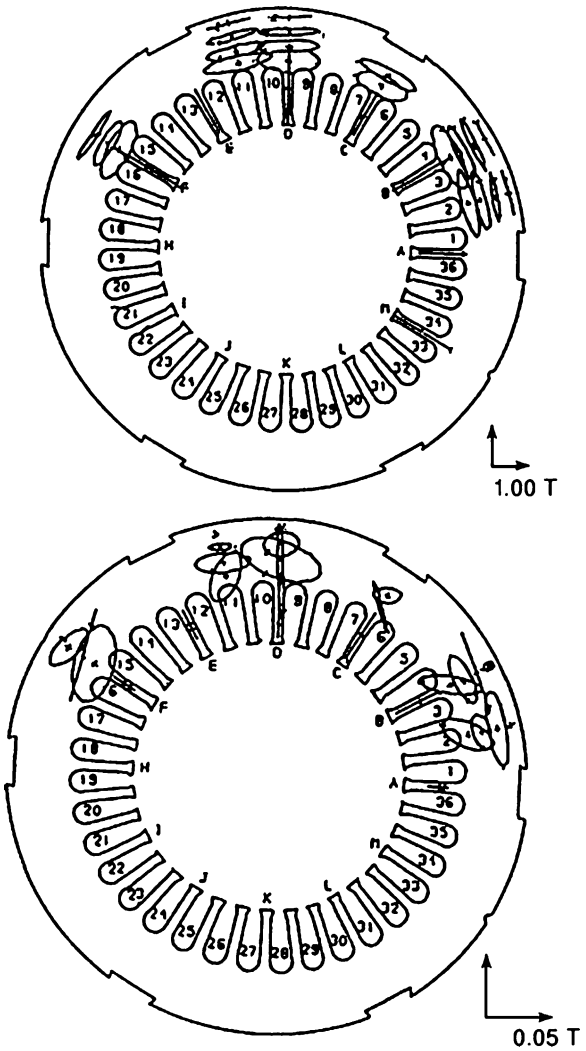

Figure 17. Loci of the localized flux density in a 3-phase induction motor stator core assembled from non-oriented silicon iron: (a) fundamental (50 Hz), (b) third harmonic (150 Hz) (core back flux density of 1.0 T) (11).

nent of flux density but the variations in the harmonic in-plane flux and the interlamina flux do cause significant localized loss changes which in turn affect the total loss by 10% to 15%. Normally, eight segments will make up a layer of the core and adjacent layers can be displaced by 22.50° or 11.25° to produce half or quarter overlap configurations. Appropriate combinations of material selection with overlap configuration lead to minimum losses. In practice in both segmented and unsegmented stator cores stress, edge burrs and insulating coating defects can lead to localized variations in the internal flux distribution causing large increases in eddy current loss which are difficult to predict or to quantify.

BIBLIOGRAPHY

1. R. Boll *Soft Magnetic Materials—The Vacuumschmelze Handbook*, London: Heyden & Jones Ltd., 1979.
2. R. M. Bozorth *Ferromagnetism*, New York: IEEE Press. 1993 (Reissue).
3. A. Goldman *Handbook of Modern Ferromagnetic Materials*, Kluwer Academic Publishers. 1999.
4. A. J. Moses Electrical steels: past, present and future developments, *IEE Proc.***137** (Pt.A, 5): 233–245, 1990.
5. T. Nozawa M. Mizogami H. Mogi Y. Matsuo Magnetic properties and dynamic domain behaviour in grain-oriented 3% SiFe, *IEEE Trans. Magn.*, **32**: 572–589, 1996.
6. J. W. Shilling G. L. Houze Magnetic properties and domain structures in grain-oriented 3% Si-Fe, *IEEE Trans. Magn.*, **M10**: 195–223, 1974.
7. F. Brailsford *Physical Principles of Magnetism*, London: Van Nostrand, 1966.

8. A. J. Moses Development of alternative magnetic core materials and incentives for their use, *J. Magn. Mag. Mat.*, **112**: 150–155, 1992.
9. I.E.C. 404-2 Methods of measurement of magnetic, electrical and physical properties of magnetic sheet and strip, 1978.
10. F. Fiorillo A. Novikov An improved approach to power losses in magnetic laminations under non-sinusoidal induction waveform; *IEEE Trans. Magn.*, **26**: 2904–2910, 1990.
11. A. J. Moses Importance of rotational losses in rotating machines and transformers, *J. Mat. Eng. Performance*, **1** (2): 236–244, 1992.
12. Y. Alinejad-Beromi A. J. Moses T. Meydan New aspects of rotating field and flux measurement in electrical steel, *J. Magn. Mag. Mat.*, **112**: 135–138, 1992.
13. A. J. Moses Effect of stresses on magnetic properties of silicon-iron laminations. *J. Mat. Sci.*, **9**: 217–222, 1974.
14. A. J. Moses P. S. Phillips Some effect of stress in Goss-oriented silicon iron, *IEEE Trans. Magn.*, 14: 353–355, 1978.
15. D. A. Ball H. O. Lorch An improved thermometric method of measuring local power dissipation, *J. Sci. Instr.*, **42**: 90–93, 1965.
16. J. J. Dalton J. Liu A. J. Moses D. H. Horrocks A. Basak A virtual instrumentation based magnetic test system. *Studies in Applied Electromagnetics and Mechanics*, **10**: 792–795, 1996.
17. A. J. Moses Classical and practical approaches to electromagnetic field solutions in magnetic devices, *Int. J. Appl. Electromagn. Mech.*, **6**: 1–8, 1995.
18. A. J. Moses Factors affecting localised flux and iron loss distribution in laminated cores, *J. Magn. Mag. Mat.*, **41**: 409–414, 1984.
19. A. J. Moses B. Thomas The spatial variation of localised power loss in two practical transformer T-joints, *IEEE Trans. Magn.*, **9**: 655–659, 1973.
20. M. A. Jones A. J. Moses J. E. Thompson Flux distribution and power loss in the mitred overlap joint in power transformer cores, *IEEE Trans. Magn.*, **9**: 114–122, 1973.
21. G. S. Radley A. J. Moses Magnetic flux and power loss in a turbogenerator, *IEEE Trans. Magn.*, **17**: 1311–1316, 1981.

A. J. MOSES
Cardiff University